Analysis of differential PDT effect in rat bladder tumor models according to concentrations of intravesical hexyl-aminolevulinate

Saoussen Berrahmoune,[a] Nicolas Fotinos,[b] Lina Bezdetnaya,[a] Norbert Lange,[b] Jean Claude Guedenet,[c] François Guillemin[a] and Marie Ange D'Hallewin[a]

Received 25th March 2008, Accepted 27th May 2008
First published as an Advance Article on the web 23rd July 2008
DOI: 10.1039/b804921a

The hexylester of 5-aminolevulinic acid (HAL) is a very efficient precursor of the photosensitizer protoporphyrin IX (PpIX) for photodynamic therapy (PDT). Our previous study, performed in rat orthotopic bladder tumors, indicated an opposite effect of HAL/PpIX-PDT according to HAL concentration. The present study investigated possible reasons for this differential effect considering the impact of extracted amounts of PpIX in normal and tumor bearing bladders along with PpIX distribution in distinctive histopathological layers. High performance liquid chromatography (HPLC) analysis of tumor and normal bladder tissues after 8 mM and 16 mM HAL instillation showed that PpIX was the main porphyrin species. The PpIX production in tumor bladders instilled with 8 mM HAL was significantly higher than after 16 mM HAL. Fluorescence confocal microscopy demonstrated a punctuate bright fluorescence pattern in tumor zones of bladders instilled with 8 mM HAL, whereas a more diffuse cytoplasmatic fluorescence distribution was observed after 16 mM HAL instillation. Immunofluorescence staining together with transmission electron microscopy showed severe mitochondrial damage in tumor zones of bladders treated with 8 mM HAL/PpIX PDT, with intact mitochondria in tumor zones of bladders treated with 16 mM HAL/PpIX PDT. We conclude that the differential response to HAL/PpIX PDT in function of HAL concentrations could be attributed to diminished PpIX synthesis and differential intracellular localisation of PpIX. Mitochondria were shown to be the critical photodamaged sites of HAL/PpIX PDT and as such tissue sensitivity to treatment can be estimated through investigation of intracellular PpIX distribution.

Introduction

Photodynamic therapy (PDT) is a treatment modality based on the cytotoxic effect occurring on target tissues by interaction of a photosensitizer with light in the presence of oxygen.[1] One of the major advances in PDT can be attributed to the use of 5-aminolevulinic acid (ALA) to induce protoporphyrin IX (PpIX) for the treatment of early stage cancers as well as diagnosis.[2,3] ALA is a precursor in the heme synthesis pathway. Exogenous ALA overcomes the negative feedback exerted by heme on endogenous ALA formation and promotes the transient formation of PpIX. Hexvix® or hexyl-aminolevulinate (HAL), a more lipophilic derivative of ALA, was approved as an adjunct to standard cystoscopy in the fluorescence diagnosis of bladder cancer in 27 European countries. Due to its higher local bioavailability, the latter allows inducing higher or identical fluorescence levels at 20 fold lower concentrations and shorter incubation times.[4,5] Fluorescence cystoscopy has been shown in large multicenter studies to enhance detection by 30%, to reduce progression by a factor 2 and to significantly reduce recurrence rate up to 8 years.[6,7]

The efficacy of ALA-PDT is determined by a variety of parameters such as intracellular localisation and concentration of PpIX at the time of treatment, optical tissue parameters, light fluence and fluence rate, oxygenation of the tissue. Our pilot study in a rat orthotopic bladder tumor model indicated a narrow therapeutic window, in which a selective HAL/PpIX-PDT effect was achieved. Complete tumor eradication, without damage to underlying tissues, was observed with 8 mM HAL and a fluence of 20 J cm^{-2} delivered at 100 mW cm^{-2}. Applying the same dosimetric parameters for 16 mM resulted in a massive wall necrosis, whereas the tumor remained intact.[8] These differential effects were observed at comparable PpIX fluorescence levels in the tumor as assessed spectroscopically *in situ.* However, fluorescence does not necessarily reflect drug concentration and considering that the amount of PpIX critically determines the sensitivity of urothelium to irradiation, PpIX extraction is warranted.[9] Another parameter, which was reported as an important determinant for photodynamic efficacy of PpIX is its subcellular localisation pattern.[10,11] The very short lifetime of singlet oxygen (10–40 ns) and resulting short diffusion length (10–20 nm), leads to the destruction of cell components only in very close vicinity of the

[a]*Photobiology in Cancerology, Centre Alexis Vautrin, CRAN Nancy University, CNRS, Avenue de Bourgogne 54511, Vandoeuvre les Nancy Cedex, France. E-mail: m.dhallewin@nancy.fnclcc.fr; Fax: +33 3 83 59 83 79; Tel: +33 3 83 59 83 06*
[b]*Department of Pharmaceutics and Biopharmaceutics, School of Pharmaceutical Sciences, University of Geneva, University of Lausanne, Geneva, Switzerland*
[c]*Department of pathology and cytology, University Hospital Nancy, Vandoeuvre-les-Nancy, France*

generation site.[12] Irradiation of cells incubated with exogenous PpIX, preferentially localized in the cell membrane or cytoplasm, induced less cell death than illumination of ALA-induced PpIX, with preferential mitochondrial localization.[10,13,14]

In the present study we undertook a mechanistic analysis of differential PDT effects in response to different HAL concentrations. Emphasis was put on two distinct parameters, HAL-induced PpIX accumulation and localization with subsequent subcellular damage.

Material and methods

Bladder cancer cell line

The tumor cell line (AY27) was initially derived from carcinomas of the urinary bladder induced in female Fischer (F344) rats continuously fed with *N*-[4-(5-nitro-2-furyl)-2-thiazolyl] formamide (FANFT). The papillary transitional AY27 cell line was primarily established by subcutaneous transplantation and subsequent maintenance in cell culture. The culture medium used was RPMI-1640 (GIBCO, Invitrogen, UK), supplemented with 10% fetal calf serum, 5% L-glutamine (200 mM) and 5% penicillin–streptomycin (Biotech, GmbH, Aidenbach, Germany). Cells were cultured in 75 cm^2 tissue culture flasks with 0.2 μm vented cup (Fisher Bioblock Scientific S.A.S, Illkirch, France) and maintained in humidified incubator with 5% CO_2 environment. At confluence, cultured cells were dissociated with 2 ml trypsin–EDTA for 10 min at 37 °C, then centrifuged and re-suspended in complemented RPMI 1640 medium. Cell viability was determined by standard trypan blue (0.4%) exclusion test.

Animal tumor model

All animal procedures were performed according to institutional and national guidelines. Female Fischer (F344) rats weighing 160–200 g were purchased from HARLAN Laboratories (Gannat, France). Animals were maintained in our animal care facility and housed four per cage at room temperature (22 ± 2 °C) with food and water *ad libidum*. The orthotopic bladder cancer model was previously described by Xiao *et al*.[15] Briefly, animals were anaesthetized with an intraperitoneal injection of 45 mg kg^{-1} sodium pentobarbital (Ceva Santé Animale, Libourne, France) and body temperature was maintained with thermostatic blanket during experiments. The rat bladders were catheterized with 16 G intravenous cannula (Terumo Surflo, Guyancourt, France). Epithelial desquamation was obtained through an intravesical instillation of 0.5 ml HCl (0.1 N) during 15 s, neutralized with 0.5 ml of NaOH (0.1 N). Bladders were washed with PBS and a bladder tumor cell suspension (0.5 ml containing 10^6 AY-27 cells) was instilled intravesically for one hour. All experiments were carried out on tumor bearing rats 10 days after tumor cell implantation.

Hexylester aminolevulinate

Solutions containing 8 or 16 mM HAL (Photocure, Oslo, Norway) were prepared by dissolving HAL powder in phosphate buffer saline (PBS). Animals were anesthetized and catheterized with a 14 G intravenous cannula (Terumo Surflo, Guyancourt, France). 0.5 ml of HAL (8 and 16 mM) was administered intravesically for one hour. Fluorescence confocal microscopy, protoporphyrin IX tissue extraction and PDT, were performed after a resting time of two and three hours for 8 and 16 mM HAL respectively, according to our previous protocol.[8]

Fluorescence confocal microscopy

Bladders of 10 rats were excised and embedded in optimal cutting temperature compound (Tissue-Tek; Sakura Finetek, Tokyo, Japan), and kept at −80 °C for one hour. Five μm frozen sections were prepared and examined under fluorescence confocal microscopy (Nikon TE2000-U microscope linked with a Biorad LRC Radiance 2100 fitted with a 100 mW argon ion laser). Excitation was performed using a 514 nm diode laser and fluorescence was collected using a ×40 dic Nikon oil immersion objective with a lateral resolution of 0,15 μm and an axial resolution of 1.52 μm. PpIX fluorescence was collected using HQ590LP filter collecting fluorescence signals above 590 nm. The final fluorescence images were constructed using photocounting process (512 × 512 pixels, 302 × 302 μm or 76 × 76 μm FOV (field of vision), 166 line per second scan).

Protoporphyrin IX tissue extraction and HPLC analysis

24 rats were used: 12 healthy rats and 12 tumor bearing rats separated in six groups. Healthy bladder controls, healthy bladders instilled with 8 mM or 16 mM HAL, bladder tumors control and bladder tumors instilled with 8 mM or 16 mM HAL. After dissection and removal of the bladders, ten μl of extraction solvent (EtOH/DMSO/acetic acid 80/20/1) was added per milligram of sample tissue. The samples were then mechanically grinded and sonicated for 15 min at 0 °C. After centrifugation for 5 min at 12 000 × *g*, the supernatant was recovered and stored at −80 °C in the dark prior to analysis. Porphyrins were analyzed by HPLC-FD, according to a modified method from Tunstall *et al.*[16] Samples were injected into a LaChrom D7000 system (Merck-Hitachi, Tokyo, Japan), equipped with a L7100 high pressure pump. Separation was carried out on an inversed phase column 125/4 Nucleodur 3 μm C18 gravity (Macherey-Nagel, Oensingen, Switzerland) protected with a corresponding precolumn. Elution was performed at a flow rate of 1 ml min^{-1} with a two-component elution. A linear gradient started with 100% of solvent A (ammonium acetate (0.5 M, pH 5.5) 90% and acetonitrile 10%) to 25% of solvent A and 75% of solvent B (methanol 90% and acetonitrile 10%) after 45 min. The solvent mixture was kept unchanged for 15 min and the column was re-equilibrated with 100% solvent A for 10 min. Porphyrins were detected with a fluorescence detector (LaChrom L-7480) with an excitation wavelength set at 407 nm and emission at 620 nm. The porphyrin concentration in the samples was determined by measuring the area under the curve and compared with standard curves. Standards used were a chromatographic marker containing the regular isomers 8- (uroporphyrin I), 7-, 6-, 5-, 4- (coproporphyrin I), and 2-carboxylate porphyrins, completed with uroporphyrin III, coproporphyrin III, zinc protoporphyrin IX and protoporphyrin IX. All porphyrin standards were purchased from Porphyrin Products (Logan, Utah, USA) and were dissolved in the prementioned extraction solvent mixture.

Whole bladder PDT

Light was delivered by an argon pumped dye laser (Spectra Physics 2020, Les Ulis, France). The optical fiber (400 μm) with a spherical light diffuser (IP159 Medlight S.A., Eccublens, Switzerland) was introduced in the bladder through a connector (Qosina, Edgewood, New York USA) screwed on a 14 G catheter. The fiber was placed in a central position in the bladder filled with 0.5 ml of sterile PBS. Irradiation was performed at a wavelength of 635 nm (20 J cm^{-2}, 100 mW cm^{-2}).

Mitochondrial damage

Mitochondrial damage was assessed by two methods: immunofluorescent marking of ATP synthase β and transmission electron microscopy. Four rats were used for each category: (i) control tumors without HAL incubation or irradiation, (ii) control tumors with irradiation only and tumor bearing bladders treated with (iii) 8 and (iv) 16 mM HAL PDT. Immediately and 4 h post-PDT, the rats were euthanized and a cystectomy was performed.

Immunofluorescence study. After cystectomy, the bladder was embedded in optimal cutting temperature compound (Tissue-Tek; Sakura Finetek, Tokyo, Japan), and kept at −80 °C until use. Blocks were cryosectioned at 5 μm thickness. Frozen sections were immediately immersed in formaldehyde 3% for fixing at room temperature for 15 min. The antibodies used for mitochondria labelling were: anti-ATP Synthase β (EC 3.6.3.14) mouse -anti -rat (Sigma, Aldrich, Saint Louis, Missouri, USA) as primary antibody and goat-anti-Mouse IgG FITC conjugate (Sigma, Aldrich, Saint Louis, Missouri, USA) as secondary antibody. The sections were rinsed three times with PBS and treated with blocking solution (5% goat serum in PBS 1×/0.3 Triton 100×) for 1 h at room temperature followed by incubation with primary antibody (5 μg ml^{-1}) overnight at 4 °C. The slides were then washed with PBS and incubated with secondary antibody diluted at 1/64 for 1 h at room temperature and then rinsed three times with PBS. Finally, the slides were mounted with fluorescent mounting medium (DakoCytomation, Glostrup, Denmark) and specimens were examined with a fluorescence microscope (Olympus AX-70, Rungis, France).

Transmission electron microscopy. Immediately after cystectomy the bladders were fixed in 2.5% glutaraldehyde in phosphate buffer 0.1 M overnight at 4 °C. Full thickness biopsies from healthy and implanted tumors were cut in thin pieces and washed 5 min with sodium cacodylate. Subsequently, they were fixed in 1% osmium tetroxide in 0.1 M phosphate buffer (pH 7.2) for 90 min and washed once again with sodium cacodylate. The samples were dehydrated through series of graded alcohol, embedded in Resin/Epon and sectioned into semi-thin sections (2 μm), which were stained with toluidine blue for pathology control. The sample was then further sectioned into ultrathin slices (75 nm) and contrasted with uranyl acetate and lead citrate and observed on a transmission electron microscope (CM10, Philips, Eindhoven, The Netherlands).

Statistical analysis

Statistical analysis was performed using unpaired *t*-tests; *p* values of less than 0.05 were considered significant.

Results

In situ fluorescence distribution of PPIX

Fig. 1 shows confocal fluorescence images of tumor bearing rat bladders two and three hours after the end of an intravesical instillation of 8 mM (Fig. 1A) or 16 mM HAL (Fig. 1B). After instillation of 8 mM HAL, transitional cell carcinoma (TCC) and healthy urothelium show the presence of bright fluorescent spots. An intravesical instillation of 16 mM HAL leads to a similar fluorescence distribution pattern in normal urothelium, whereas transformed AY27 epithelium exhibits a more diffuse fluorescence. At both HAL concentrations, the fluorescence intensity of PpIX in muscle was barely detectable.

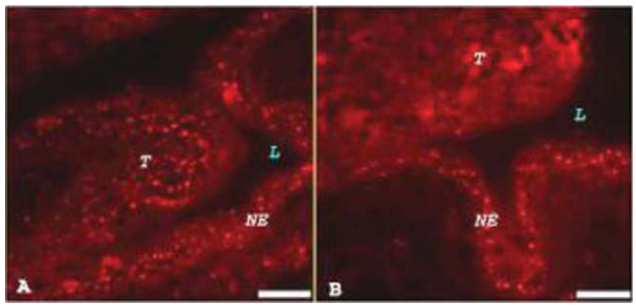

Fig. 1 Confocal fluorescence microscopy obtained from tumor bearing bladder sensitized with 8 (A) and 16 mM HAL (B) showing fluorescence distribution (L: lumen, T: tumor and NE: normal epithelium). Bar = 50 μm.

HPLC-assessed tissue extraction of PpIX and its metabolites

Application of two HAL concentrations on tumor bladders resulted in accumulation of PpIX along with related metabolites (Fig. 2A). PpIX was the main detected porphyrin species, whereas the amount of all other metabolites was very low and never exceeded 0.06 nmol (g tissue)$^{-1}$. Similar contents of PpIX pro-metabolites were recorded in healthy bladders subjected to both HAL concentrations (data not shown). PpIX concentrations in healthy bladders were not significantly different after instillation with 8 and 16 mM of HAL (2.06 *vs.* 2.86, $p > 0.05$) (Fig. 2B). Likewise, no statistically significant difference was found between tumor bladders instilled with 16 mM HAL and healthy bladders, irrespective of the HAL ($p > 0.05$) (Fig. 2B). However, the PpIX production in tumor bladders instilled with 8 mM HAL was higher than that after 16 mM HAL (7.52 nmol g^{-1} *vs.* 4.72 nmol g^{-1}; $p < 0.05$) (Fig. 2B).

Photodamaged sites

Mitochondrial damage in tumor bearing bladders was probed by immunofluorescent staining of mitochondrial ATP synthase β. ATP synthase is a transmembrane protein responsible for driving the reversible reaction from ADP + phosphate to ATP.[17] Its β-subunit is located in the peripheral stalk. Using fluorescence labelled anti-ATP synthase β, intact mitochondria are revealed as fluorescence spots as shown in frozen section of untreated tumor (Fig. 3A) and muscle (Fig. 3D). Immediately after 8 and 16 mM HAL-PDT, the mitochondrial staining pattern remained

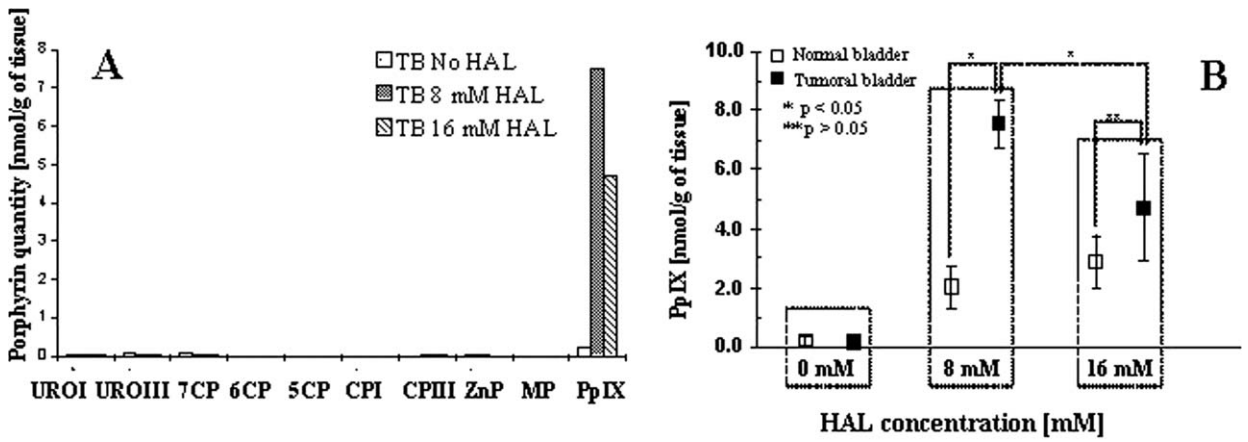

Fig. 2 Porphyrin profile expressed in nmol g^{-1} of tissue extracted *ex vivo* from tumor bladders (TB) non-instilled and instilled with two HAL concentration separated by HPLC-FD; (URO I: uroporphyrin I, URO III: uroporphyrin III, 7CP, 6CP, 5CP: 7-, 6-, 5-carboxylate porphyrins, MP: mesoporphyrin, CPI: coproporphyrin I, CPIII: coproporphyrin III, ZnP: zinc protoporphyrin IX, PpIX: protoporphyrin IX) (A). PpIX quantity extracted from normal □ and tumor bearing ■ bladders in control animals (no drug) and after 8 and 16 mM HAL instillation, measured by HPLC-FD (B).

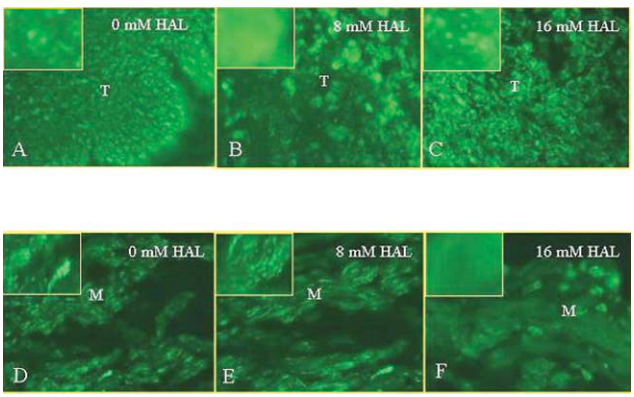

Fig. 3 Immunofluorescence staining with ATP synthase β (×40). A: tumor zone of untreated bladder; B: tumor zone of bladder treated with 8 mM HAL-PDT; C: tumor zone of bladder treated with 16 mM HAL-PDT; D: muscle of untreated bladder; E: muscle of tumor bladder treated with 8 mM HAL-PDT, F: muscle of tumor bladder treated with 16 mM HAL-PDT. Inserted are magnifications of single cells. Sections of tumor bearing bladders were observed at 4 h post-PDT ($\lambda = 635$ nm, fluence = 20 J cm^{-2}, fluence rate = 100 mW cm^{-2}). (T: tumor, M: muscle).

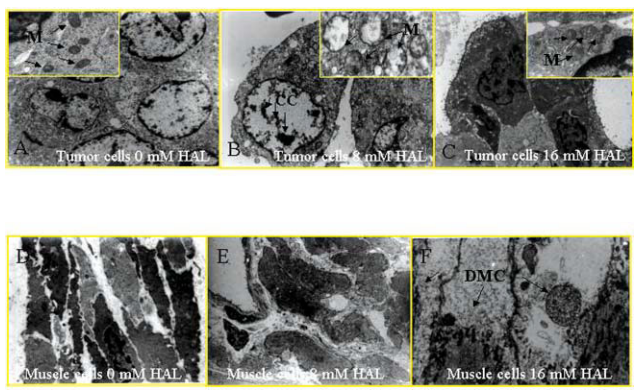

Fig. 4 Transmission electron microscopy of tumor-bearing bladders sections observed at 4 h post-PDT ($\lambda = 635$ nm, fluence = 20 J cm^{-2}, fluence rate = 100 mW cm^{-2}). A: tumor cells of untreated bladder (×2.95 K); insert: enlarged image (×15.5 K) of intact mitochondria (M). B: tumor cells of bladder treated with 8 mM HAL-PDT (×5.2 K); insert: enlarged image (×28.5 K) of altered mitochondria (M) and chromatin condensation (CC). C: tumor cells of bladder treated with 16 mM HAL-PDT (×2.2 K); insert: enlarged image (×15.5 K) of intact mitochondria (M). D: myocytes of untreated tumor bearing bladder (×5.2 K), E: myocytes of tumor bladder treated with 8 mM HAL-PDT (×5.2 K). F: damaged myocytes (DMC) of bladder treated with 16 mM HAL-PDT (×5.61 K).

unchanged (data not shown). Four hours post-PDT with 8 mM HAL, the fluorescence pattern becomes diffuse in the tumor compartment of bladders (Fig. 3B) while the muscularis remains punctuated (Fig. 3E). In contrast, the fluorescence aspect in the tumor of bladders after 16 mM HAL-PDT was punctuated (Fig. 3C) whereas that of the bladder muscle was diffuse (Fig. 3F).

Transmission electron micrographs of tumor bladders treated with 8 and 16 mM HAL-PDT are displayed in Fig. 4. No signs of tumoral nor muscular damage were observed in non-irradiated bladders (Fig. 4A, 4D). No abnormalities were noticed immediately after 8 or 16 mM HAL-PDT (data not shown). Four hours after the addition of 8 mM HAL-PDT, we observed damage in AY27 cells of bladders (Fig. 4B) together with intact muscle cells (Fig. 4E). Alterations of tumor cells treated with 8 mM HAL-PDT (Fig. 4B) consisted in chromatin condensation and mitochondrial damage with crest ruptures, vacuoles and swelling (insert to Fig. 4B). Tumor cells of bladders treated with 16 mM HAL-PDT remain intact even 4 h post-PDT (Fig. 4C) whereas completely destroyed myocytes (Fig. 4F) were noted at the same conditions.

Discussion

In a previous study we have optimised HAL-PpIX based photodynamic treatment of bladder cancer in an orthotopic rat bladder tumor model.[8] Among several tested HAL concentrations and light doses, we have found conditions that resulted in an inverted PDT effect on tumor and muscle. This opposite effect was obtained at similar HAL-induced PpIX fluorescence levels of the mucosal layer as measured non-invasively *in situ*.

In order to introduce a mechanistic aspect of this selective PDT effect, we focused our present investigation on two parameters: the extracted amounts of HAL-induced PpIX in normal and tumor bearing bladders and the PpIX distribution in distinctive histopathological layers of the bladder and successive photodamage.

The HPLC profiles of porphyrin metabolites of healthy and tumor bladders at both HAL concentrations (8 and 16 mM) showed that the main porphyrin species was PpIX (Fig. 2A). Further, HPLC results clearly demonstrated that the PpIX amount of tumor bearing bladders instilled with 8 mM HAL was higher than healthy bladder instilled with both HAL concentrations (8 and 16 mM) as well as tumor bearing bladders instilled with 16 mM HAL (Fig. 2B). This differential PpIX accumulation between tumor bearing and healthy bladders is consistent with the difference in metabolising ability of the porphyrin-heme biosynthetic pathway between cancerous and normal cells and/or increased permeability of tumor cells for HAL.[18,19] HPLC analysis was performed on whole bladder extracts, thus with an intermingling input from both tumor and muscle compartment. Since healthy bladders produced an identical amount of PpIX, irrespective of pro-drug concentration, it is reasonable to assume that the reduced amount of PpIX in whole bladder extracts after 16 mM compared to 8 mM is due to reduced tumoral PpIX synthesis. PpIX synthesis is known to be critically dependent on initial pro-drug concentration. There is a threshold after which a reduction of the PpIX quantity is observed. Steinbach *et al.* demonstrated *in vitro* a linear correlation between the concentration of ALA and the fluorescence intensity of PpIX up to a certain ALA concentration, after which a plateau was observed.[20] He *et al.* reported a linear increase of PpIX accumulation in human dermal microvascular endothelial cells (HMEC-1) after incubation with a certain range of HAL concentrations, followed by decline at higher pro-drug concentrations.[21] The same tendency was reported in an *in vivo* study in pig bladders and in human oesophagus: increasing the ALA dose leads to increasing PpIX production up to a certain point, after which PpIX levels remain stable.[22–23] In a clinical pilot study of photodetection of bladder cancers with HAL, Lange *et al.* observed that PpIX generation is positively correlated with low HAL concentrations (4 and 8 mM) while instillation with 16 mM resulted in less PpIX accumulation.[4]

The decrease in the amount of PpIX observed in our study could be attributed to several mechanisms related to heme biosynthesis. Esterase activity, which is responsible for hydrolysis of HAL to ALA is probably not the limiting step since the kinetics of porphyrin synthesis from ALA esters are comparable to ALA in almost all tissues.[24] Increasing the pro-drug concentration and, thus, increasing intracellular ALA content, can in turn cause inhibition of rate-limiting enzymes of the heme biosynthesis pathway such as porphobilinogen synthase and porphobilinogen deaminase (PBGD) (EC 4.3.1.8).[25] The inhibition of these critical enzymes induces a deviation of heme biosynthesis pathway which causes the cytoplasmic porphyrin synthesis. However, PBGD activity seems to play a minor role for the differential accumulation of PpIX in urothelial cells.[26] Another possibility could be related to a saturation of benzodiazepine receptor (PBR), responsible for the transport of cytoplasmic coproporphyrinogen III to mitochondria where the transformation to protoporphyrin IX takes place, thus leading to a diminution of PpIX.[27,28] Additional experiments establishing a specific binding of coproporphyrinogen III to PBR upon our conditions are needed to verify this hypothesis.

Another parameter, which is of paramount importance for photodynamic efficacy is the pro-drug induced PpIX intratissular and intracellular localization.[13,29] Fluorescence confocal microscopy images demonstrated a punctuate bright fluorescence patterns in tumor zones of bladders instilled with 8 mM HAL (Fig. 1A), whereas a more diffuse cytoplasmatic fluorescence distribution was observed after 16 mM HAL instillation (Fig. 1B). Considering that endogenous PpIX biosynthesis takes place in mitochondria, we have assumed a mitochondrial PpIX accumulation after 8 mM HAL. Since PpIX–mitochondrial colocalisation studies are technically impossible on frozen sections, we have studied mitochondrial PpIX localisation indirectly, through the detection of photodamaged sites. Mitochondrial photodamage was assessed by immunofluorescence staining of anti-ATP Synthase β and electron microscopy. Fluorescence labeling of mitochondria showed fluorescent spots in tumor zones of untreated bladders (Fig. 3A). Four hours after 8 mM HAL-mediated PDT, the pattern becomes diffuse in the tumor, indicating disruption of the mitochondrial membrane (Fig. 3B). This observation is consistent with tumor necrosis as assessed by HES staining in our previous study.[8] Alternatively, four hours after 16 mM HAL-PDT, the fluorescence pattern in the tumor zone remained punctiform (Fig. 3C), corresponding to intact tumor as observed on pathology slides.[8]

Electron microscopic observation of bladder tumors four hours after PDT confirmed results of immunofluorescence. After 8 mM HAL-PDT, we observed tumor cell alterations with mitochondrial damage and chromatin condensation (Fig 4B, insert 4B) corresponding to apoptotic features of cell death. We have inspected other intracellular organelles (endoplasmic reticulum, Golgi apparatus; data not shown) and mitochondria appeared to be the only photodamaged site. Sixteen mM HAL-PDT failed to induce mitochondrial or any other damage in the tumors (Fig 4C, insert 4C), whereas muscle destruction was confirmed. We thus conclude that the punctiform fluorescence image observed on confocal microscopy of frozen sections of bladder tumors instilled with 8 mM HAL (Fig 1A) is consistent with mitochondrial-PpIX localisation and that these organelles can be considered as critical photodamage sites.

Another issue that should be discussed in relation to localization is a time-dependent migration of mitochondrial PpIX to cytoplasm followed by cellular efflux.[13,30,31] Accordingly, PDT efficacy is the highest at shorter incubation times and decreases gradually with longer light drug intervals (LDI).[13] Our PDT experiments were performed after one hour incubation with the pro-drug, followed by two or three hours resting time for 8 mM and 16 mM HAL respectively. The different LDIs were chosen in order to obtain a comparable PpIX fluorescence for both initial HAL concentrations.[8] Indeed, incubation of tumor bearing bladders with 8 mM HAL and adding one resting hour (to reach an LDI of $1 + 3 = 4$) does not alter the fluorescence distribution, with persistence of bright spots (data not shown). Neither does reducing the LDI by one hour (to reach $1 + 2 = 3$) in case of tumor bearing bladders instilled with 16 mM HAL alter the fluorescence pattern, which remains diffuse (data not shown). Therefore, in our particular case, the time factor is not responsible for differential intracellular localization. Efflux of the prodrug itself could also

be an issue. Indeed, it has been shown that ALA and HAL very quickly leave the cells, and this efflux is proportional to the intracellular content.[32]

It would be very appealing if similar to tumor, PpIX localization in muscle could also stand for the selective PDT effect. However, the present study does not provide sufficient evidence for this conclusion, thus warranting further investigations.

Clinical PDT has not gained widespread acceptance in the oncology community at this moment. Technical complexity and skin toxicity can be partly held responsible for this phenomenon. The major issue however might be the variable response of patients, treated under identical conditions. It is therefore of the utmost importance to establish parameters that can be applied to predict treatment outcome. Furthermore, these parameters have to be detectable by minimally invasive techniques. From the present study, it appears that subcellular localization and concentration of PpIX can both be used to predict treatment outcome in rat bladder cancers. Concentration measurements however cannot be performed non-invasively. Alternatively, confocal fiberoptic fluorescence microscopy can be successfully performed in rat bladders *in vivo*.[33] This tool could thus potentially be used to visualize PpIX distribution in bladder tumors and predict treatment outcome.

Abbreviations

PDT	Photodynamic therapy
HAL	Hexyl-aminolevulinate
ALA	5-Aminolevulinic acid
PpIX	Protoporphyrin IX
FANFT	*N*-[4-(5-Nitro-2-furyl)-2-thiazolyl] formamide
HPLC	High Performance Liquid Chromatography

Acknowledgements

This work was supported by a grant from the French Cancer Ligue "La ligue contre le cancer". We thank Photocure ASA for supplying Hexvix®. Technical assistance by Sami El Khatib, Jacques Didelon, Valérie Legué, Agnes Leroux, and François Plénat is also gratefully acknowledged.

References

1 T. J. Dougherty, Photodynamic therapy, *Clin. Chest Med.*, 1985, **6**, 219–236.
2 M. Kriegmair, R. Baumgartner, R. Knuechel, P. Steinbach, A. Ehsan, W. Lumper, F. Hofstadter and A. Hofstetter, Fluorescence photodetection of neoplastic urothelial lesions following intravesical instillation of 5-aminolevulinic acid, *Urology*, 1994, **44**, 836–841.
3 M. Kriegmair, R. Baumgartner, W. Lumper, R. Waidelich and A. Hofstetter, Early clinical experience with 5-aminolevulinic acid for the photodynamic therapy of superficial bladder cancer, *Br. J. Urol.*, 1996, **77**, 667–671.
4 N. Lange, P. Jichlinski, M. Zellweger, M. Forrer, A. Marti, L. Guillou, P. Kucera, G. Wagnieres and H. van den Bergh, Photodetection of early human bladder cancer based on the fluorescence of 5-aminolaevulinic acid hexylester-induced protoporphyrin IX: a pilot study, *Br. J. Cancer*, 1999, **80**, 185–193.
5 A. Marti, P. Jichlinski, N. Lange, J. P. Ballini, L. Guillou, H. J. Leisinger and P. Kucera, Comparison of aminolevulinic acid and hexylester aminolevulinate induced protoporphyrin IX distribution in human bladder cancer, *J. Urol.*, 2003, **170**, 428–432.
6 E. Hungerhuber, H. Stepp, M. Kriegmair, C. Stief, A. Hofstetter, A. Hartmann, R. Knuechel, A. Karl, S. Tritschler and D. Zaak, Seven years' experience with 5-aminolevulinic acid in detection of transitional cell carcinoma of the bladder, *Urology*, 2007, **69**, 260–264.
7 S. Denzinger, M. Burger, B. Walter, R. Knuechel, W. Roessler, W. F. Wieland and T. Filbeck, Clinically relevant reduction in risk of recurrence of superficial bladder cancer using 5-aminolevulinic acid-induced fluorescence diagnosis: 8-year results of prospective randomized study, *Urology*, 2007, **69**, 675–679.
8 S. El Khatib, J. Didelon, A. Leroux, L. Bezdetnaya, D. Notter and M. D'Hallewin, Kinetics, biodistribution and therapeutic efficacy of hexylester 5-aminolevulinate induced photodynamic therapy in an orthotopic rat bladder tumor model, *J. Urol.*, 2004, **172**, 2013–2017.
9 L. Vaucher, P. Jichlinski, N. Lange, C. Ritter-Schenk, H. van den Bergh and P. Kucera, Hexyl-aminolevulinate-mediated photodynamic therapy: how to spare normal urothelium. An *in vitro* approach, *Lasers Surg. Med.*, 2007, **39**, 67–75.
10 Z. Ji, G. Yang, V. Vasovic, B. Cunderlikova, Z. Suo, J. M. Nesland and Q. Peng, Subcellular localization pattern of protoporphyrin IX is an important determinant for its photodynamic efficiency of human carcinoma and normal cell lines, *J. Photochem. Photobiol., B*, 2006, **84**, 213–220.
11 F. Wierrani, D. Fiedler, G. Schnitzhofer, J. C. Stewart, K. Gharehbaghi, M. Henry, W. Grin, W. Grunberger and B. Krammer, A new approach to cancer therapy due to appropriate uptake and retention kinetics of *meta*-tetrahydroxy-phenylchlorin in a human fibroblast cell line, *Cancer Biochem. Biophys.*, 1996, **15**, 171–176.
12 J. Moan and K. Berg, The photodegradation of porphyrins in cells can be used to estimate the lifetime of singlet oxygen, *Photochem. Photobiol.*, 1991, **53**, 549–553.
13 B. C. Wilson, M. Olivo and G. Singh, Subcellular localization of Photofrin and aminolevulinic acid and photodynamic cross-resistance in vitro in radiation-induced fibrosarcoma cells sensitive or resistant to photofrin-mediated photodynamic therapy, *Photochem. Photobiol.*, 1997, **65**, 166–176.
14 B. Krammer and K. Uberriegler, *In vitro* investigation of ALA-induced protoporphyrin IX, *J. Photochem. Photobiol., B*, 1996, **36**, 121–126.
15 Z. Xiao, T. J. McCallum, K. M. Brown, G. G. Miller, S. B. Halls, I. Parney and R. B. Moore, Characterization of a novel transplantable orthotopic rat bladder transitional cell tumour model, *Br. J. Cancer*, 1999, **81**, 638–646.
16 R. G. Tunstall, A. A. Barnett, J. Schofield, J. Griffiths, D. I. Vernon, S. B. Brown and D. J. Roberts, Porphyrin accumulation induced by 5-aminolaevulinic acid esters in tumour cells growing *in vitro* and *in vivo*, *Br. J. Cancer*, 2002, **87**, 246–250.
17 J. A. Leyva, M. A. Bianchet and L. M. Amzel, Understanding ATP synthesis: structure and mechanism of the F1-ATPase (Review), *Mol. Membr. Biol.*, 2003, **20**, 27–33.
18 Y. Ohgari, Y. Nakayasu, S. Kitajima, M. Sawamoto, H. Mori, O. Shimokawa, H. Matsui and S. Taketani, Mechanisms involved in delta-aminolevulinic acid (ALA)-induced photosensitivity of tumor cells: relation of ferrochelatase and uptake of ALA to the accumulation of protoporphyrin, *Biochem. Pharmacol.*, 2005, **71**, 42–49.
19 J. Moan, O. Bech, J. M. Gaullier, T. Stokke, H. B. Steen, L. W. Ma and K. Berg, Protoporphyrin IX accumulation in cells treated with 5-aminolevulinic acid: dependence on cell density, cell size and cell cycle, *Int. J. Cancer*, 1998, **75**, 134–139.
20 P. Steinbach, H. Weingandt, R. Baumgartner, M. Kriegmair, F. Hofstadter and R. Knuchel, Cellular fluorescence of the endogenous photosensitizer protoporphyrin IX following exposure to 5-aminolevulinic acid, *Photochem. Photobiol.*, 1995, **62**, 887–895.
21 D. He, S. Behar, N. Nomura, S. Sassa and H. W. Lim, The effect of ALA and radiation on porphyrin/heme biosynthesis in endothelial cells, *Photochem. Photobiol.*, 1995, **61**, 656–661.
22 J. F. B. H. J. Van Staveren, C. W. Verlaan, A. Edixhoven, T. M. de Reijke, G. Brutel de la and R. G. a. W. M. Sta, Comparison of normal piglet bladder damage after PDT with oral or intravesical administration of ALA., *Lasers Med. Sci.*, 2006, **17**, 238.
23 C. J. Kelty, R. Ackroyd, N. J. Brown, S. B. Brown and M. W. Reed, Comparison of high- *vs* low-dose 5-aminolevulinic acid for photodynamic therapy of Barrett's esophagus, *Surg. Endosc.*, 2004, **18**, 452–458.
24 G. Di Venosa, A. Batlle, H. Fukuda, A. Macrobert and A. Casas, Distribution of 5-aminolevulinic acid derivatives and induced porphyrin kinetics in mice tissues, *Cancer Chemother. Pharmacol.*, 2006, **58**, 478–486.

25 L. Greenbaum, D. J. Katcoff, H. Dou, Y. Gozlan and Z. Malik, A porphobilinogen deaminase (PBGD) Ran-binding protein interaction is implicated in nuclear trafficking of PBGD in differentiating glioma cells, *Oncogene*, 2003, **22**, 5221–5228.
26 R. C. Krieg, S. Fickweiler, O. S. Wolfbeis and R. Knuechel, Cell-type specific protoporphyrin IX metabolism in human bladder cancer *in vitro*, *Photochem. Photobiol.*, 2000, **72**, 226–233.
27 S. Taketani, H. Kohno, T. Furukawa and R. Tokunaga, Involvement of peripheral-type benzodiazepine receptors in the intracellular transport of heme and porphyrins, *J. Biochem.*, 1995, **117**, 875–880.
28 M. Mesenholler and E. K. Matthews, A key role for the mitochondrial benzodiazepine receptor in cellular photosensitisation with delta-aminolaevulinic acid, *Eur. J. Pharmacol.*, 2000, **406**, 171–180.
29 R. Sailer, W. S. Strauss, M. Wagner, H. Emmert and H. Schneckenburger, Relation between intracellular location and photodynamic efficacy of 5-aminolevulinic acid-induced protoporphyrin IX *in vitro*. Comparison between human glioblastoma cells and other cancer cell lines, *Photochem. Photobiol. Sci.*, 2007, **6**, 145–151.
30 S. Iinuma, S. S. Farshi, B. Ortel and T. Hasan, A mechanistic study of cellular photodestruction with 5-aminolaevulinic acid-induced porphyrin, *Br. J. Cancer*, 1994, **70**, 21–28.
31 S. Sandberg, I. Romslo, G. Hovding and T. Bjorndal, Porphyrin-induced photodamage as related to the subcellular localization of the porphyrins, *Acta Derm. Venereol. Suppl. (Stockholm)*, 1982, **100**, 75–80.
32 G. Di Venosa, H. Fukuda, A. Batlle, A. MacRobert and A. Casas, Photodynamic Therapy: regulation of porphyrin synthesis and hydrolysis from ALA esters, *J. Photochem. Photobiol., B*, 2006, **83**, 129–136.
33 M. A. D'Hallewin, S. El Khatib, A. Leroux, L. Bezdetnaya and F. Guillemin, Endoscopic confocal fluorescence microscopy of normal and tumor bearing rat bladder, *J. Urol.*, 2005, **174**, 736–740.

